

A family-based method of quantifying NEOWISE diameter errors

Joseph R. Masiero¹, A.K. Mainzer¹, E.L. Wright²

ABSTRACT

Quantifying the accuracy with which physical properties of asteroids can be determined from thermal modeling is critical to measuring the impact of infrared data on our understanding of asteroids. Previous work (Mainzer *et al.* 2011b) has used independently-derived diameters (from asteroid radar, occultations, and spacecraft visits) to test the accuracy of the NEOWISE diameter determinations. Here, we present a new and different method for bounding the actual NEOWISE diameter errors in the Main Belt based on our knowledge of the albedos of asteroid families. We show the 1σ relative diameter error for the Main Belt population must be less than 17.5% for the vast majority of objects. For a typical uncertainty on H magnitude of 0.2 mag, the relative error on diameter for the population would be $\sim 10\%$.

1. Introduction

Asteroid families are composed of objects formed from the catastrophic breakup of a single, larger parent body (Masiero *et al.* 2015; Michel *et al.* 2015; Nesvorný *et al.* 2015). For objects that have not undergone partial- or total-differentiation, it is reasonable to assume that the original parent had a macroscopically homogeneous composition, and that each member of the family represents a single, independent sample of this composition (Michel *et al.* 2015). Similarly, as asteroid family members are all the same age (with the caveat that a small fraction of members may have undergone later impact events) and reside in nearly the same location in the Solar system, we can assume that any evolution of the surface (e.g. due to space weathering) affects all members in the same fashion (Nesvorný *et al.* 2015). Thus, by measuring a particular property for many family members we can better quantify the true value of the original parameter that is being sampled. In this work, we use the average and variance of the albedos measured for all members of an asteroid family ($\widehat{p_V}$, $\sigma_{\widehat{p_V}}^2$) as an estimator for the true albedo (p_V).

¹Jet Propulsion Laboratory/California Institute of Technology, 4800 Oak Grove Dr., MS 183-301, Pasadena, CA 91109, USA, Joseph.Masiero@jpl.nasa.gov

²University of California, Los Angeles, CA, 90095

2. Relationship between errors on diameter, absolute magnitude, and albedo

Asteroid albedo (p_V) and diameter (D) are related through the absolute magnitude (H) by the equation (Harris & Lagerros 2002):

$$D_{km} = 1329 \frac{10^{-H/5}}{\sqrt{p_V}} \quad (1)$$

The H magnitude is derived from a fit to the observed visible light apparent magnitudes, often using an assumed phase curve slope parameter G (Bowell *et al.* 1989). Diameter is determined through a thermal model fit to measured infrared emitted fluxes. Albedo is then inferred from these two parameters. The uncertainty on an albedo measurement will therefore derive from the uncertainties on the diameter as measured by e.g. NEOWISE, and the uncertainty on the H magnitude. The H magnitude uncertainty is driven by the uncertainty in the apparent magnitude measurements from ground-based telescopes as well as by the assumed phase curve slope parameter G .

By converting Equation 1 from absolute magnitude to an effective flux (F_H) and propagating the uncertainty (σ) on each of these parameters, we find that:

$$\sqrt{p_V} = C_1 \frac{\sqrt{2.511^{-H}}}{D} \quad (2)$$

$$p_V = C_2 \frac{F_H}{D^2} \quad (3)$$

$$\left(\frac{\sigma_{p_V}}{p_V}\right)^2 = \left(\frac{\sigma_{F_H}}{F_H}\right)^2 + \left(\frac{2\sigma_D}{D}\right)^2 - 2\frac{\sigma_{DF_H}}{DF_H} \quad (4)$$

where where C_1 and C_2 are constants and σ_{DF_H} is the covariance between diameter and the H magnitude. As H is based on reflected visible light measurements and D is based on emitted thermal infrared fluxes, the measurements are independent and $\sigma_{DF_H} = 0$.

In the case where we have an independent measurement of the fractional error on albedo, we can use the relationship in Equation 4 to determine the maximum possible error on either diameter or H magnitude by assuming the error on the other is zero. This is of course unphysical, but allows us to determine the worst-case scenario for the errors on one parameter. Thus, if the H magnitude is perfectly known ($\sigma_{F_H} = 0$), the error on diameter and albedo will be directly correlated. For non-zero values of σ_{F_H} , the albedo error is a combination of the H and D errors. This therefore sets an upper limit on the diameter error from a measurement of the albedo error of:

$$\frac{\sigma_D}{D} < 0.5 \frac{\sigma_{p_V}}{p_V}. \quad (5)$$

Therefore, a quantification of the fractional uncertainty on an albedo determination for a population ($\sigma_{\widehat{pV}}$) sets an upper limit on the fractional uncertainty for the diameter determination of that population.

We note that propagating the error using Equation 1 as written will result in a term that includes the covariance of albedo and absolute magnitude. As all of the albedos used for this study were determined through thermal modeling and visible light H magnitude fitting, albedo and H are not independent, and the covariance between these two parameters is large and significant.

3. Asteroid families as tests of albedo and diameter errors

With asteroid families, we effectively have a series of independent measurements of the same surface. As objects were not known *a priori* to be a family member when they were observed by NEOWISE (Mainzer *et al.* 2011a) or when physical properties were determined (Masiero *et al.* 2011), and because the objects were detected over a wide range of observing geometries and sky positions, there are no correlated systematic errors that can affect one family without affecting the entire catalog. Thus, families act as a method of independent verification of the quality of the thermal model fits. The albedos of objects with common spectral taxonomy could also be used in a similar fashion (e.g. Mainzer *et al.* 2011c). However, it is conceivable that a selection effect mechanism could induce a separate systematic error, as albedo and taxonomy both are driven by optical reflectance properties. Family membership, conversely, is established by orbital dynamics (Nesvorný *et al.* 2015), in particular the time-integrated proper orbital elements. For this work, we use the most recent asteroid family list from the Planetary Data System (PDS, Nesvorný 2015).

It is important to note that family membership lists are now often filtered by albedo following the release of the NEOWISE physical property measurements to remove interlopers (e.g. Masiero *et al.* 2013; Milani *et al.* 2014). This is because the Main Belt has a bimodal albedo distribution (Masiero *et al.* 2011) and interlopers from the other compositional complex can be easily identified. Although this could potentially result in a decrease in the scatter in the albedo measurements, in practice it is not applied with this level of precision and instead acts only as a coarse cut to remove objects with grossly inconsistent compositions. The principal outlier in this process is the Nysa-Polana family complex, which is known to consist of at least two overlapping families of different compositions (Cellino *et al.* 2002; Masiero *et al.* 2011, 2015), but is still listed as a single entry in PDS. For this reason, we have removed the Nysa-Polana complex from consideration in this work.

The results of Anderson-Darling tests of normality for the albedo distributions of each family show that the null hypothesis of normality cannot be rejected at the $p = 0.05$ probability level for one-third of the families. We note that the Anderson-Darling test is particularly sensitive to differences in the tails of the distribution from a normal distribution. For the families where the null hypothesis could be rejected, comparison of the cumulative distribution functions of the

albedos and the best-fit Gaussian show the albedo distributions typically are narrower than the low wing but broader than the high wing of the Gaussian. This is likely due to the fact that some of the uncertainties on the parameters that contribute to albedo do not follow a normal distribution. For example, the uncertainty on apparent magnitude due to unknown rotational phase will follow a sinusoidal distribution, and light curve maxima will be better measured than minima in a magnitude-limited survey. This would result in an overestimate of the brightness, and thus a skew to higher albedos, as is observed. Thus, while the albedos of some families do not follow a precise normal distribution, the width of the best-fit Gaussian provides a useful metric for characterizing the systematics encountered in asteroid thermal modeling.

4. Results

We show in Figures 1 and 2 the fractional width of the albedo distributions for asteroid families as a function of distance from the sun, and mean family albedo. This fractional width is the 1σ spread of the best-fit Gaussian to the albedo distribution divided by the mean albedo of the family ($w = \frac{\sigma_{pV}}{pV}$). We plot each family that has more than 50 albedo measurements in the NEOWISE data set (Mainzer *et al.* 2016). In total we use 35,468 asteroids for this analysis.

We separately analyze only those objects that had a fitted beaming parameter in the NEOWISE data set. The beaming parameter of the NEATM thermal model was allowed to vary when an observation included two thermally dominated channels, and accounts for uncertainties in the model and physical properties of the object (Mainzer *et al.* 2011b). Of the 137,014 unique MBAs with published NEOWISE-derived parameters, 65,323 have fitted beaming values, while the others were assumed to be a fixed value during fitting (Masiero *et al.* 2011, 2012). As they are a smaller population, we calculate the fractional width for all families with more than 20 albedo measurements from fitted-beaming diameter determinations. In total 20,150 asteroids with fitted beaming were used here.

We note that this is a parallel analysis to what is published in Masiero *et al.* (2015). There, the authors quote the standard deviation of the mean of the albedo distribution, which represents the accuracy with which the mean albedo is known, and decreases linearly with the number of objects measured. The spread of the distribution, being the width of the Gaussian fit, should remain constant for any peak value as long as the sample size is sufficient.

We list our measured w values for all family members used and only those family members with fitted beaming values in Table 1, along with the numbers of objects used for each family. Our measurements show that the typical spread for family albedos is 20% – 35%, with a characteristic value of 27%. All but two families have a fractional width of $w < 40\%$. This means that the maximum possible uncertainty on NEOWISE diameter measurements for family members is 20%, with the vast majority below $\sim 17.5\%$. The true diameter uncertainty is significantly lower as this assumes that the H magnitudes are perfectly known, whereas in reality H magnitudes are known to

have errors of order 0.2 mag, or $\sim 20\%$ in flux (Pravec *et al.* 2012; Vereš *et al.* 2015). If we consider only the objects with fitted beaming values, we find that the w measurements decrease slightly, as does the characteristic spread for all families. This also confirms that the assumed beaming parameters used for fits with only a single thermal band are appropriate for the population.

Previous works (e.g. Masiero *et al.* 2011) have used the log of the albedo as a primary diagnostic quantity. As a test, we have performed a parallel analysis of the distribution of $\log p_V$ for each family. We find a comparable rate of success and failure of the Anderson-Darling normality test for the log-distributions, and the measured widths of the best-fit gaussians match those in Table 1 when translated to linear-space. As the use of logarithms adds another layer of complexity to the error-propagation, we prefer to use the linear-albedo distributions here, but both produce comparable results.

Errors on diameter determination come from two primary sources: the measurement uncertainties on the fluxes that are used for thermal modeling, and difference between the simplified model of the asteroid’s thermal behavior and the actual thermal behavior of the surface. A single measurement at SNR= 5 will have a 20% uncertainty on infrared flux which translates to a 20% uncertainty on surface area, and thus $\sim 10\%$ uncertainty diameter. As the number of detection and SNR of detections increases, this component of the error diminishes. The NEOWISE object detection pipeline required five observations with SNR > 4.5, for a total SNR ~ 10 . Therefore, the majority of the uncertainty on diameter derives from the differences between the thermal model used and the reality of the asteroid surface, and that is the uncertainty we are constraining with the test described here.

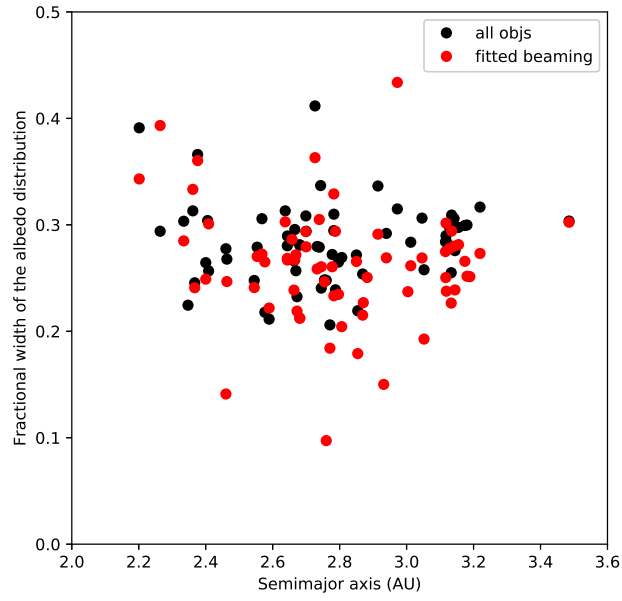


Fig. 1.— Fractional width of the albedo distribution ($w = \frac{\sigma_{\widehat{p_V}}}{\widehat{p_V}}$) for the 65 families with more than 50 measured albedos (black), as a function of distance to the Sun. Red points show the fractional width of only objects with fitted beaming parameters, for 68 families with more than 20 measured albedos.

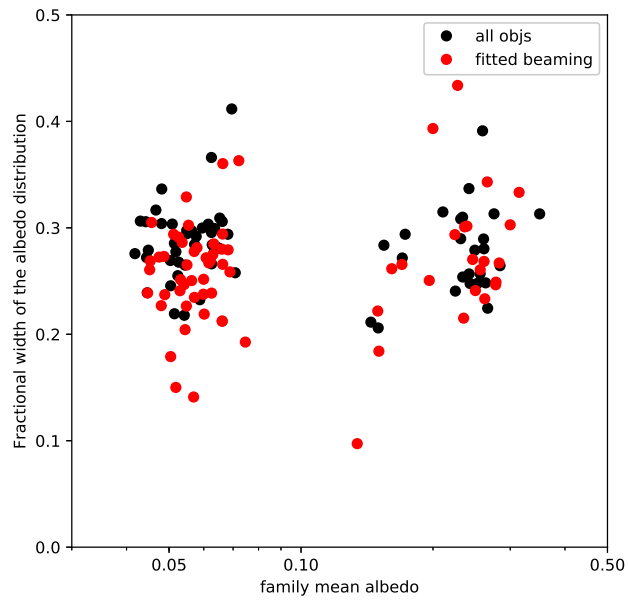


Fig. 2.— The same as Fig 1 but compared to the mean albedo of the family (\widehat{p}_V).

5. Conclusions

The diameter errors for NEOWISE as told by asteroid families are bounded to be less than 17.5% for the vast majority of objects assuming perfect knowledge of the H magnitude, and certainly lower when the uncertainty on the H magnitude is taken into account. If the assumption that the composition of family members is homogeneous is not correct, then natural variations will inflate the width of the albedo distribution, and this will further lower the upper limit on diameter accuracy. A 1σ uncertainty of 10% in diameter and 0.2 mags in H magnitude will result in a 28% uncertainty on the albedo determination, which corresponds to the average dispersion we measure for all families. An over-estimation of diameter uncertainty from a theoretical case can occur when the assumptions about the input physical parameters are allowed to vary beyond values supported by reality. Mathematical solutions to many equations are possible that are contradicted by data from the physical world. We therefore use data-based interpretations when available to quantify the real-world NEOWISE modeling uncertainties.

Acknowledgments: We thank both referees for comments that led to clarifications, refinements, and improvements to this manuscript, as well as the editor Melissa McGrath for helping shepherd this through the referee process. This research was carried out at the Jet Propulsion Laboratory, California Institute of Technology, under a contract with the National Aeronautics and Space Administration. This publication makes use of data products from the Wide-field Infrared Survey Explorer, which is a joint project of the University of California, Los Angeles, and the Jet Propulsion Laboratory/California Institute of Technology, funded by the National Aeronautics and Space Administration. This publication also makes use of data products from NEOWISE, which is a project of the Jet Propulsion Laboratory/California Institute of Technology, funded by the Planetary Science Division of the National Aeronautics and Space Administration.

REFERENCES

- Bowell, E., Hapke, B., Domingue, D., Lumme, K., Peltoniemi, J. & Harris, A.W., 1989, Asteroids II, University of Arizona Press, 524.
- Cellino, A., Bus, S.J., Doressoundiram, A., Lazzaro, D., Asteroids III, W. F. Bottke Jr., A. Cellino, P. Paolicchi, and R. P. Binzel (eds), University of Arizona Press, 633.
- Harris, A.W. & Lagerros, J.S.V., Asteroids III, W. F. Bottke Jr., A. Cellino, P. Paolicchi, and R. P. Binzel (eds), University of Arizona Press, 205.
- Mainzer, A.K., Bauer, J.M., Grav, T., Masiero, J., Cutri, R.M., Dailey, J., Eisenhardt, P., McMillan, R.M. *et al.*, 2011a, ApJ, 731, 53.
- Mainzer, A.K., Grav, T., Masiero, J., Bauer, J.M., Wright, E., Cutri, R.M., McMillan, R.S., Cohen, M., Ressler, M., Eisenhardt, P., 2011b, ApJ, 736, 100.

- Mainzer, A.K., Grav, T., Masiero, J., *et al.*, 2011c, *ApJ*, 741, 90.
- Mainzer, A.K., Bauer, J., Cutri, R., Grav, T., Kramer, E., *et al.*, 2016, NASA Planetary Data System, EAR-A-COMPIL-5-NEOWISEDIAM-V1.0.
- Masiero, J.R., Mainzer, A.K., Grav, T., Bauer, J.M., *et al.*, 2011, *ApJ*, 741, 68.
- Masiero, J.R., Mainzer, A., Bauer, J., Grav, T., Nugent, C., Stevenson, R., 2013, *ApJ*, 770, 7.
- Masiero, J.R., Grav, T., Mainzer, A.K., Nugent, C., Bauer, J., Stevenson, R., Sonnett, S., 2014, *ApJ*, 791, 121.
- Masiero, J.R., DeMeo, F.E., Kasuga, T., Parker, A.H., 2015, *Asteroids IV*, P. Michel, F.E. DeMeo, W.F. Bottke (eds), University of Arizona Press, 323.
- Michel, P., Richardson, D., Durda, D., Jutzi, M., Asphaug, E., 2015, *Asteroids IV*, P. Michel, F.E. DeMeo, W.F. Bottke (eds), University of Arizona Press, 341.
- Milani, A., Cellino, A., Knežević, Z., Novaković, B., Spoto, F., Paolicchi, P., 2014, *Icarus*, 239, 46.
- Nesvorný, D., Brož, M., Carruba, V., 2015, *Asteroids IV*, P. Michel, F.E. DeMeo, W.F. Bottke (eds), University of Arizona Press, 297.
- Nesvorný, D., 2015, EAR-A-VARGBDET-5-NESVORNYFAM-V3.0, NASA Planetary Data System.
- Pravec, P., Harris, A.W., Kušnirák, P., Galád, A. & Hornoch, K., 2012, *Icarus*, 221, 365.
- Vereš, P., Jedicke, R., Fitzsimmons, A., Denneau, L., Granvik, M. *et al.*, 2015, *Icarus*, 261, 34.

Table 1:: Fractional width of the albedo distribution (w) measured for families from all members with albedo measurements, and only those with fitted beaming values (w_{beam}). The number of family members used is listed (N) as well as the family name and ID number from the PDS table (Nesvorný 2015). Families with insufficient numbers of objects ($N < 50$ for all members or $N < 20$ fitted beaming values) are listed as ‘n/a’.

Family ID	Name	w	N	w_{beam}	N_{beam}
401	Vesta	0.31	1853	0.33	542
402	Flora	0.39	3008	0.34	1204
403	Baptistina	0.29	646	0.39	233
404	Massalia	0.26	246	0.30	33
406	Erigone	0.25	806	0.24	404
407	Clarissa	0.30	67	n/a	n/a
408	Sulamitis	0.27	170	0.25	97
410	Euterpe	0.22	57	n/a	n/a
413	Klio	0.30	320	0.28	197
414	Chimaera	0.28	72	0.14	49
415	Chaldaea	0.37	126	0.36	86
501	Juno	0.26	218	0.27	76
502	Eunomia	0.28	2069	0.27	1166
504	Nemesis	0.29	396	0.28	165
505	Adeona	0.23	1335	0.22	896
506	Maria	0.28	954	0.27	425
507	Padua	0.28	582	0.26	317
509	Chloris	0.41	133	0.36	83
510	Misa	0.29	310	0.29	149
512	Dora	0.26	803	0.23	543
513	Merxia	0.24	99	0.26	27
514	Agnia	0.31	114	0.23	44
515	Astrid	0.24	220	0.29	68
516	Gefion	0.25	640	0.25	283
517	Konig	0.31	235	0.27	114
518	Rafita	0.25	242	0.24	81
519	Hoffmeister	0.27	967	0.26	440
522	Ino	0.34	81	n/a	n/a
528	Leonidas	0.28	68	0.21	50
529	Vibilia	0.28	68	0.21	50
530	Phaео	0.29	136	0.33	93
531	Mitidika	0.27	635	0.24	446
532	Henan	0.31	144	0.29	49
533	Hanna	0.27	116	0.20	54
534	Karma	0.22	77	0.27	45
535	Witt	0.25	75	n/a	n/a
537	Watsonia	n/a	n/a	0.10	32
541	Postrema	0.28	65	0.31	43
601	Hygiea	0.31	2067	0.28	1396
602	Themis	0.31	2186	0.29	1624
603	Sylvia	0.30	151	0.30	99
604	Meliboea	0.28	270	0.24	205
605	Koronis	0.25	1053	0.22	587
606	Eos	0.28	3726	0.26	2197
607	Emma	0.31	310	0.27	220
608	Brasilia	0.27	115	0.27	41
609	Veritas	0.30	678	0.27	410
611	Naema	0.29	231	0.27	156
612	Tirela	0.29	282	0.30	116
613	Lixiaohua	0.28	510	0.24	367

Table 1:: Fractional width of the albedo distribution (w) measured for families from all members with albedo measurements, and only those with fitted beaming values (w_{beam}). The number of family members used is listed (N) as well as the family name and ID number from the PDS table (Nesvorný 2015). Families with insufficient numbers of objects ($N < 50$ for all members or $N < 20$ fitted beaming values) are listed as ‘n/a’.

Family ID	Name	w	N	w_{beam}	N_{beam}
614	Telramund	0.31	83	0.43	22
617	Theobalda	0.30	172	0.25	122
618	Terentia	n/a	n/a	0.15	23
622	Terpsichore	0.22	81	0.18	54
623	Fringilla	0.34	102	0.29	81
625	Yakovlev	n/a	n/a	0.23	29
626	Sanmarcello	n/a	n/a	0.25	23
630	Aegle	0.26	71	0.19	58
631	Ursula	0.30	891	0.28	720
632	Elfriede	n/a	n/a	0.25	29
638	Croatia	0.26	104	0.23	68
641	Juliana	n/a	n/a	0.24	24
701	Phocaea	0.26	740	0.25	344
801	Pallas	0.21	64	0.18	47
803	Hansa	0.29	354	0.27	123
804	Gersuind	0.21	138	0.22	51
805	Barcelona	0.31	87	0.30	21
807	Brucato	0.30	263	0.27	220
901	Euphrosyne	0.30	1476	0.28	1097
902	Alauda	0.28	977	0.27	858
904	Luthera	0.32	133	0.27	110
905	Armenia	n/a	n/a	0.25	24